

Photodissociation and recombination of solvated I_2^- : What causes the transient absorption peak?

N. Delaney, J. Faeder, and R. Parson^{a)}

JILA, National Institute of Standards and Technology and Department of Chemistry and Biochemistry, University of Colorado, Boulder, Colorado 80309-0440

(Received 14 April 1999; accepted 5 May 1999)

Using nonadiabatic molecular dynamics simulations, we present evidence that the 2 ps peak in the pump-probe spectrum of I_2^- dissociated inside CO_2 clusters is due to transitions from the ground state to the spin-orbit excited states, rather than to excited-state absorption as previously assigned.

© 1999 American Institute of Physics. [S0021-9606(99)02426-5]

I. INTRODUCTION

Seven years ago, Lineberger and co-workers observed evidence of coherent nuclear motion in the photodissociation and recombination of I_2^- clustered with CO_2 .¹⁻³ In their experiment, a 720 nm pulse excites the I_2^- chromophore to its repulsive A' state (Fig. 1). Dissociation of the chromophore makes the cluster transparent, allowing recombination to be monitored with a subsequent 720 nm probe pulse. Since the excited clusters dispose of their excess energy by evaporation, the mass spectrum of the ionic photofragments enables one to identify those clusters which have absorbed both pulses. By measuring the intensity of this two-photon product channel as a function of time delay between pump and probe, Lineberger and co-workers determined the overall time scale for dissociation, recombination, and vibrational relaxation of the solvated ion. The most striking result of these experiments was a transient peak in the absorption recovery at about 2 ps after excitation, which was attributed to the coherent passage of recombining chromophores through a region of the potential surface characterized by strong absorption. A similar feature has been seen in the dissociation and recombination of I_2^- in liquid solutions.^{4,5}

These experiments have stimulated an intensive program of research into the dynamics of I_2^- photodissociation and recombination. Pump-probe experiments have now been carried out on a variety of clusters^{6,7} as well as liquid solutions.^{4,5,8,9} Measurements of the absorption recovery in particular mass channels¹⁰ have yielded information about the dynamics of the solvent cage during the recombination process. Femtosecond time-resolved photoelectron spectra (FPES)^{11,12} have provided complementary insights into the mechanisms of recombination and relaxation in these systems. Finally, nonadiabatic molecular dynamics simulations have successfully reproduced the experimental product distributions,¹³⁻¹⁶ time-resolved photoelectron spectra,¹⁷ and the overall absorption recovery,¹⁸ and have led to a detailed molecular picture of the dynamics.

A crucial element is missing from the picture, however: the mechanism that gives rise to the 2 ps transient peak in the

absorption recovery has never been conclusively identified. Lineberger and co-workers originally ascribed it to absorption from the inner wall of the weakly bound A state to the higher-lying a state (Fig. 1). This assignment is consistent with the polarization dependence of the signal, which shows that the associated transition moment is parallel to the internuclear axis, and with the solution-phase experiments, which found that the transient disappeared when the system was probed with UV radiation.⁵ The FPES experiments¹² and the simulations^{15,16,18} did find significant A -state recombination, but in the simulations the A -state dynamics was observed to be diffusive rather than coherent, and the trajectories did not appear to find regions where the $A \rightarrow a$ transition might be resonant with the probe. Instead, the simulations found that a significant fraction of the ensemble recombined in the *ground* state on this time scale. This suggests that the transient might be due to ground-state absorption, but this could not be demonstrated directly since the simulation statistics were not sufficient to resolve the finer structures in the absorption recovery.¹⁸

In this communication we present new simulation results which, we believe, settle this issue. By using a much larger number of trajectories than earlier studies, we are able to resolve the 2 ps transient in the absorption recovery and to show that it is due to transitions from the ground state to the *spin-orbit excited* B and a' states of I_2^- . The absorption occurs at large internuclear distances ($R > 3.7$ Å), as the fragments first recombine, not at the inner turning point. This possibility was considered by Papanikolas *et al.*,^{2,3} but tentatively ruled out because it requires that the spin-orbit energy be efficiently converted into thermal energy of the cluster in order to yield the observed two-photon fragments. The subsequent experimental^{7,19} and theoretical²⁰ demonstration that spin-orbit quenching is actually extremely efficient in these systems, occurring on a time scale of a few ps, removes this objection. Our new assignment is consistent with the parallel probe transition moment observed in the clusters, and with the absence of a 2 ps transient in the UV probe absorption. Analysis of the simulations using an electron-transfer perspective described in previous work^{15,16,20} shows that solvent-induced perturbations of the solute electronic struc-

^{a)} Author to whom correspondence should be addressed. Electronic mail: rparson@jila.colorado.edu

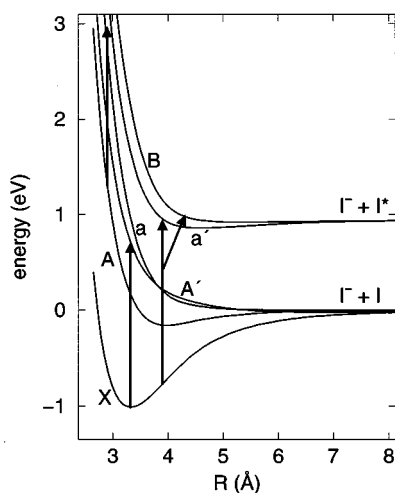


FIG. 1. Scaled *ab initio* gas phase potential curves for I_2^- . Arrows mark the 720 nm pump absorption ($X \rightarrow A'$), our assignment of the transient absorption peak at 2 ps ($X \rightarrow a'$, B), and a previous assignment for the same ($A \rightarrow a$).

ture play a crucial role in determining the regions of strong absorption.

II. METHODS

The simulations are based on an effective Hamiltonian discussed in detail elsewhere.^{16,21} The interaction between the I_2^- solute and the rigid CO_2 solvent molecules is represented by an operator that includes state-dependent electrostatic and induction interactions based on *ab initio* calculations of the solute electronic structure²² and experimental data for the solvent charge distribution and polarizability. The one-electron density matrix derived from the solute wave functions is expanded in distributed multipole operators.²³ Diagonal elements of these operators describe the solute charge density in various electronic states, while off-diagonal elements describe transition charge densities that allow the solvent to polarize the solute charge density. In the present application these distributed transition moments are also used to assemble the transition dipole matrix elements that determine the optical absorption intensities. State-independent atom-atom Lennard-Jones potentials, fit to reproduce known $I^- - CO_2$ and $I - CO_2$ potential curves,²⁴ account for the dispersion and repulsion interactions between solute and solvent, while the $CO_2 - CO_2$ interaction potential is taken from Murthy *et al.*²⁵ The overall model captures the sensitive dependence of the solute charge distribution on the solute electronic state, the solute bond length, and the positions and orientations of the solvent molecules. At each trajectory time step the Hamiltonian matrix, which depends parametrically upon the coordinates of all the solute and solvent nuclei, is constructed and diagonalized, yielding the energies, forces, and nonadiabatic transition probabilities required to proceed to the next step. Nuclear motion on a single adiabatic potential surface is computed using the velocity version of the Verlet algorithm, while hopping between surfaces is computed using a modified version¹⁶ of Tully's MDQT method.^{26,27}

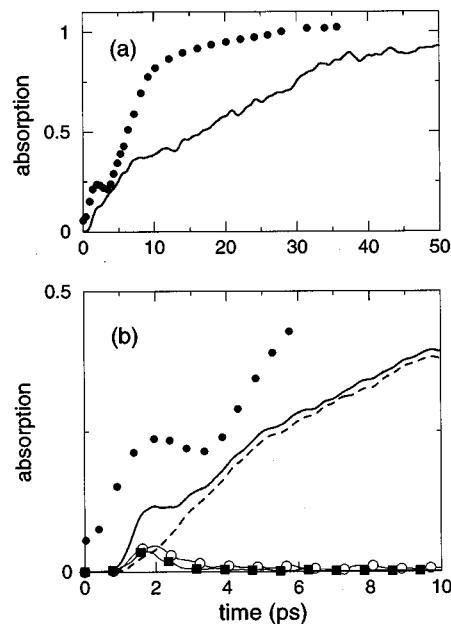


FIG. 2. Absorption recovery of $I_2^- CO_{16}$. (a) Comparison of experimental (dots) and simulated (line) signals. Simulated signal is from 100-trajectory ensemble and reaches its asymptotic value between 60 and 80 ps. (b) Solid line is the total simulated signal from a 250-trajectory ensemble, dots are the experimental data. Dashed line is the contribution from the $X \rightarrow A'$ transition. The transient feature at 2 ps is due to $X \rightarrow a'$ and $X \rightarrow B$ transitions, shown, respectively, by the open circles and filled squares.

The absorption recovery signal is calculated using the quasiclassical prescription of Coker and co-workers.^{18,28} Along each trajectory, a contribution to the probe absorption is recorded when the energy gap between the occupied state and a higher-lying state falls within a Gaussian window around the probe frequency; these contributions are weighted by the square of the transition dipole moment connecting these states. In addition, the signal is convoluted with a Gaussian pulse in time. In the results reported here the time width $\sigma_t = 150$ fs, consistent with the experimental value of ≈ 120 fs (Ref. 2), and the energy width $\sigma_E = 0.005$ a.u. (Ref. 29). These simulations required much larger trajectory ensembles than our earlier study of the final product distributions,¹⁵ because only a small portion of the ensemble contributes to the absorption signal in a particular time window. For each cluster size studied, 250 trajectories were computed from starting configurations obtained by sampling a single 2.5 ns trajectory with an average temperature of 80 K. The dissociation and recombination times vary from a few picoseconds to over 75 ps in some cases where I_2^- is temporarily trapped in an excited electronic state. Since we are primarily interested in short time dynamics most of the simulations were terminated at 20 ps, although we did run one ensemble of 100 trajectories out to 100 ps in order to establish the asymptotic behavior. To compensate for the smaller size of this ensemble, the time width, σ_t , was increased to 300 fs.

III. RESULTS AND DISCUSSION

In Fig. 2 we compare our simulated absorption recovery signal with the experiments of Papanikolas *et al.*^{2,30} The

simulation clearly reproduces the transient absorption feature at 2 ps. We have found the transient in two separate 250-trajectory simulations of $I_2^-(CO_2)_{16}$ photodissociated at 720 nm, in a simulation using a lower pump frequency (790 nm), and in simulations of I_2^- clustered with 10, 12, and 14 CO_2 molecules. The feature is less distinct in the smaller clusters, in agreement with experiment. The intensity of the 2 ps bump relative to the overall absorption recovery is lower in the simulation than in the experiment, but this is hard to interpret since the measured two-photon product signal depends on photofragment branching ratios as well as the transition moments for probe absorption; for now we make only qualitative comparisons.³¹

While the short-time dynamics is well reproduced, Fig. 2(a) shows that at longer times the absorption recovery is significantly slower in the simulations than in the experiment. Margulis and Coker found a similar discrepancy in their simulation,¹⁸ and attributed it to trajectories that become trapped in the intermediate *A* state for long times before relaxing to the ground state. *A*-state trapping was also seen in our own previous study,¹⁶ in which we calculated the time-dependent state populations but not the absorption recovery. While the FPES experiments of Neumark and co-workers provide evidence that *A*-state recombination does indeed occur,¹² the associated spectral features disappear in a few ps, implying that both simulations underestimate the rate of *A*→*X* electronic quenching. Since the two simulation models are constructed in very different ways, we infer that the disagreement with experiment is due to some physical approximation common to both, such as the neglect of intramolecular CO_2 vibrations, rather than to incidental details of the potentials.

In Fig. 2(b) we decompose the total absorption according to the final states involved in the transitions. While the overall rise is dominated by absorption from the ground state to the *A'* excited state (the same transition that initially dissociated the molecule), the 2 ps transient is entirely due to transitions from the ground state to the *a'* and *B* excited states, which correlate to spin-orbit excited iodine (I^*). Although the *A* state is populated, transitions originating on this state make a negligible contribution to the signal, because trajectories on the *A* state never find regions where such transitions would be resonant at 720 nm. By varying the probe frequency in our simulations, we have found that the strong *A*→*a* transition does begin to contribute to the absorption signal at wavelengths longer than about 1100 nm. This suggests that the *A*-state population could be monitored by probing the system with infrared radiation, which could provide information about the *A*→*X* quenching rate complementary to that derived from the FPES experiments.

To further elucidate the origin of the 2 ps peak, we map the trajectories using two coordinates: *R*, the solute bondlength, and $\Delta\Phi$, a collective solvent coordinate defined as the change in energy when a unit charge is moved from one I atom to the other holding all nuclear coordinates fixed. The magnitude of $\Delta\Phi$ is small for symmetric solvent configurations around the solute, and large for asymmetric configurations in which one I atom is preferentially solvated. We monitor *R* and $\Delta\Phi$ along the simulation trajectories and

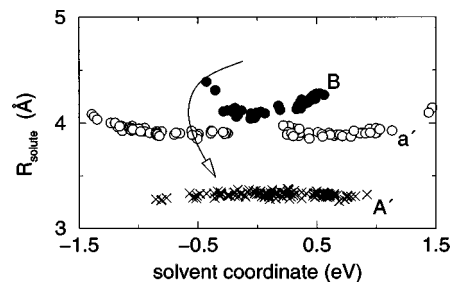


FIG. 3. Location of strong, 720 nm absorption regions in the (*R*, $\Delta\Phi$) plane. Transitions originate on the *X* state and end on the *A'* (\times 's), *a'* (open circles), and *B* (filled circles) states. Arrow represents simplified pathway for trajectories recombining on the *X* state.

record those points for which the contribution of the trajectory to the probe absorption exceeds a threshold value. The resulting plot, Fig. 3, displays the solute and solvent configurations that give rise to the various components of the probe absorption. The *X*→*A'* transitions occur primarily near the equilibrium bond distance, confirming the view that the overall absorption recovery is due to recombination followed by vibrational relaxation on the ground state. The transitions to the spin-orbit excited *a'* and *B* states occur at larger internuclear distances, as I_2^- recombines. Since both the *X* and *a'* states have *ungerade* symmetry in the isolated molecule, the *X*→*a'* transition is forbidden at $\Delta\Phi=0$ but becomes allowed in highly asymmetric solvent environments. The *X*→*B* transition, in contrast, is strongest in symmetric environments. A more extensive analysis of the influence of the solvent on the probe absorption spectrum will be included in a future publication.

Figures 2 and 3 lead to a physical picture for the photodissociation/recombination process that ties together the insights derived from earlier studies. After dissociation, some members of the ensemble temporarily recombine on the *A* state, while others hop directly to the ground state in less than 2 ps.^{16,18} As I and I^- recombine on the *X* state, they pass through the strong *X*→(*a'*,*B*) absorption region at $R=3.7$ – 4.5 Å. This initial coherent passage gives rise to the 2 ps transient peak. Since the recombined I_2^- loses energy very readily to the solvent, particularly near the top of the ground state well,^{5,32,33} it never returns to the large-*R* absorption region, so the transient is not repeated. Instead, the solute relaxes vibrationally, giving rise to the main *X*→*A'* absorption recovery. This vibrational relaxation, which is accompanied by a loss of coherence in the ensemble, is very rapid; we estimate a vibrational lifetime of about 3.8 ps near the bottom of the *X*-state well, which is very similar to the 3–6 ps lifetimes found in liquid solutions.^{5,32} In contrast, the time scale for electronic quenching of the *A* state is tens of picoseconds in the simulations. At longer times the simulated absorption recovery is therefore dominated by the slow transfer of population from the *A* state to the *X* state, rather than by *X*-state vibrational relaxation.¹⁸ Since the simulations appear to underestimate the *A*-state quenching rate, it is likely that in the experiment the time scales are less well separated, so that both electronic and vibrational relaxation contribute to the absorption recovery.

In summary, our simulations provide strong evidence that the 2 ps peak in the absorption recovery signal is due to transitions from the ground state to the spin-orbit excited states of I_2^- , not to transitions originating on the intermediate A state. The transient absorption occurs as the photofragments first begin to recombine, rather than at the inner turning point, and is strongly influenced by the solvent environment. This reassignment is consistent with all of the experimental evidence, and reinforces the physical picture of the recombination dynamics that has emerged from earlier simulations.

ACKNOWLEDGMENTS

We thank Carl Lineberger, John Papanikolas, Paul Maslen, Andrei Sanov, Sreela Nandi, Charles Qian, David Coker, Dan Neumark, and Paul Barbara for stimulating discussions and for preprints of unpublished work. This work was supported by the National Science Foundation under Grant CHE-9873742 and by the National Center for Supercomputing Applications (NCSA) under Grant CHE970015N for computing time on the SGI CRAY Origin2000 at the NCSA, University of Illinois at Urbana-Champaign.

- ¹J. Papanikolas, V. Vorsa, M. Nadal, P. Campagnola, J. Gord, and W. Lineberger, *J. Chem. Phys.* **97**, 7002 (1992).
- ²J. Papanikolas, V. Vorsa, M. Nadal, P. Campagnola, H. Buchenau, and W. Lineberger, *J. Chem. Phys.* **99**, 8733 (1993).
- ³J. M. Papanikolas, I_2^- Photodissociation and Cage Recombination Dynamics in Size-Selected $I_2^-(CO_2)_n$ Clusters, Ph.D. thesis, University of Colorado, 1994.
- ⁴D. A. V. Klinier, J. C. Alfano, and P. F. Barbara, *J. Chem. Phys.* **98**, 5375 (1993).
- ⁵P. K. Walhout, J. C. Alfano, K. A. M. Thakur, and P. F. Barbara, *J. Phys. Chem.* **99**, 7568 (1995).
- ⁶V. Vorsa, S. Nandi, P. J. Campagnola, M. Larsson, and W. C. Lineberger, *J. Chem. Phys.* **106**, 1402 (1997).
- ⁷S. Nandi, A. Sanov, N. Delaney, J. Faeder, R. Parson, and W. C. Lineberger, *J. Phys. Chem. A* **102**, 8827 (1998).
- ⁸A. E. Johnson, N. E. Levinger, and P. F. Barbara, *J. Phys. Chem.* **96**, 7841 (1992).
- ⁹G. Ashkenazi, U. Banin, A. Bartana, R. Kosloff, and S. Ruhman, *Adv. Chem. Phys.* **100**, 317 (1997).
- ¹⁰A. Sanov, S. Nandi, and W. C. Lineberger, *J. Chem. Phys.* **108**, 5155 (1998).
- ¹¹B. J. Greenblatt, M. T. Zanni, and D. M. Neumark, *Science* **276**, 1675 (1997).
- ¹²B. J. Greenblatt, M. T. Zanni, and D. M. Neumark, *Faraday Discuss.* **108**, 101 (1997).
- ¹³V. S. Batista and D. F. Coker, *J. Chem. Phys.* **106**, 7102 (1997).
- ¹⁴J. Faeder, N. Delaney, P. E. Maslen, and R. Parson, *Chem. Phys. Lett.* **270**, 196 (1997).
- ¹⁵N. Delaney, J. Faeder, P. E. Maslen, and R. Parson, *J. Phys. Chem. A* **101**, 8147 (1997).
- ¹⁶J. Faeder, N. Delaney, P. E. Maslen, and R. Parson, *Chem. Phys.* **239**, 525 (1998).
- ¹⁷J. Faeder and R. Parson, *J. Chem. Phys.* **108**, 3909 (1998).
- ¹⁸C. Margulis and D. F. Coker, *J. Chem. Phys.* **110**, 5677 (1999).
- ¹⁹A. Sanov, T. Sanford, S. Nandi, and W. C. Lineberger, *J. Chem. Phys.* **111**, 664 (1999), this issue.
- ²⁰N. Delaney, J. Faeder, and R. Parson, *J. Chem. Phys.* **111**, 651 (1999), this issue.
- ²¹P. E. Maslen, J. Faeder, and R. Parson, *Mol. Phys.* **94**, 693 (1998).
- ²²P. E. Maslen, J. Faeder, and R. Parson, *Chem. Phys. Lett.* **263**, 63 (1996).
- ²³A. J. Stone, *The Theory of Intermolecular Forces* (Oxford, New York, 1996).
- ²⁴Y. Zhao, C. C. Arnold, and D. M. Neumark, *J. Chem. Soc., Faraday Trans.* **89**, 1449 (1993).
- ²⁵C. S. Murthy, S. F. O'Shea, and I. R. McDonald, *Mol. Phys.* **50**, 531 (1983).
- ²⁶J. C. Tully, *J. Chem. Phys.* **93**, 1061 (1990).
- ²⁷S. Hammes-Schiffer and J. C. Tully, *J. Chem. Phys.* **101**, 4657 (1994).
- ²⁸V. S. Batista and D. F. Coker, *J. Chem. Phys.* **106**, 6923 (1997).
- ²⁹While this is larger than the value $\sigma_E=0.001$ a.u. derived from the spectral bandwidth in the femtosecond experiments of Papanikolas *et al.* (Ref. 2), we find that varying σ_E from 0.0001 to 0.005 a.u. has only minor effects on the essential spectral features. The larger value effectively smoothes the simulated absorption signal.
- ³⁰We compare to the "magic angle" absorption recovery, Fig. 9(a) of Ref. 2, in which the effects of cluster rotation have been removed by averaging the two absorption signals measured with the probe parallel and perpendicular to the pump. This is the appropriate signal with which to compare our simulation, because our calculated absorption intensities do not take into account the orientation of the transition dipole in the laboratory frame.
- ³¹We have normalized the simulated absorption signal in Fig. 2(b) by scaling the intensity at 20 ps to match the intensity, at 20 ps, of the normalized absorption recovery signal calculated using the 100-trajectory, long-time ensemble, Fig. 2(a). This indirect procedure is required because the 250-trajectory ensemble used to generate Fig. 2(b) was terminated at 20 ps, before the signal had reached its asymptotic limit.
- ³²I. Benjamin, P. F. Barbara, B. J. Gertner, and J. T. Hynes, *J. Phys. Chem.* **99**, 7557 (1995).
- ³³J. M. Papanikolas, P. E. Maslen, and R. Parson, *J. Chem. Phys.* **102**, 2452 (1995).